Codeposition of zirconium with aluminium from $AlBr_3$-dimethylethylphenylammonium bromide solutions in toluene

Algimantas Stakėnas, Leonas Simanavičius, Albertas Šarkis and Eimutis Matulionis

Institute of Chemistry, A. Goštauto 9, LT-2600 Vilnius, Lithuania

Zirconium and aluminium codeposition has been investigated in the $AlBr_3$-dimethylethylphenylammonium bromide melt solutions in toluene with addition of zirconium salts. The electrodeposits were found to contain from several hundredth up to 15 wt. % of zirconium. The extremely close deposition potentials of both metals were noticed. The diffusion coefficient for zirconium ions were determined to be about one order of magnitude less than of aluminium.

Key words: codeposition, zirconium, aluminium, voltammetry, nonaqueuos solutions, dimethylethylphenylammonium bromide

INTRODUCTION

The developing micro- and nanotechnology requires various thin metallic layers with particular, peculiar properties which can be achieved electrodepositing alloys of less common metals [1].

There have been reports on electrodeposition of a number of transition metals – aluminium binary alloys, *e.g.* Co–Al [2–6], Cr–Al [7–9], Mn–Al [10], Ni–Al [2, 11], Ti–Al [12] and some others.

As has been indicated recently [8], zirconium alloys with aluminium form metallic glasses, *i.e.* valuable metastable alloys of a single phase.

Codeposition of zirconium with aluminium is also of considerable theoretical interest. As is known, the redox potential of zirconium in aqueous solutions is one of those closest to that of aluminium (–1.529 and –1.676 V, respectively [13]). Redox potentials of metals in organic systems are generally brought still closer; furthermore, for instance, the redox potential of manganese is even more negative as compared to aluminium [8]. Electrochemical properties of zirconium in organic solutions are poorly known, and any studies on codeposition of zirconium with aluminium are lacking at all.

In this article, we describe the results of an investigation of the codeposition of zirconium with aluminium from the $AlBr_3$-dimethylethylphenylammonium bromide (DMEPAB) melt solutions in toluene with the addition of zirconium salts.

EXPERIMENTAL

Preparation of DMEPAB and aluminium electrolyte, electrochemical measurements and analysis of electrodeposits obtained are described elsewhere [9].

Zirconium (IV) acetylacetonate [$Zr(Acac)_4$] for synthesis (Merck-Schuchardt) and acetylacetone (2,4 pentadione) of reagent grade (Reakhim) were used. ZrF_4, $ZrCl_4$, $ZrCr_4$ and ZrJ_4 were synthesized and purified as described in [14].

RESULTS AND DISCUSSION

As illustrated in Fig. 1, voltammetric measurements in $AlBr_3$-DMEPAB melt solutions in toluene with the addition of $Zr(Acac)_4$ show that only a single reduction wave appears in the potential range of about minus 0.10–0.20 V *vs* Al(III)/Al. However, microanalysis data showed that the electrodeposits obtained in $AlBr_3$-DMEPAB solutions containing various zirconium salts consisted of aluminium and zirconium. As may be seen from Table, zirconium content in deposits increases clearly with increasing the zirconium salt concentration in the electrolyte. The deposit composition seems to depend also on the constitution of zirconium salt, that is, on the nature of the anion.

At the same time zirconium content in deposits decreases with increasing the current density, what would be expected when the zirconium standard re-

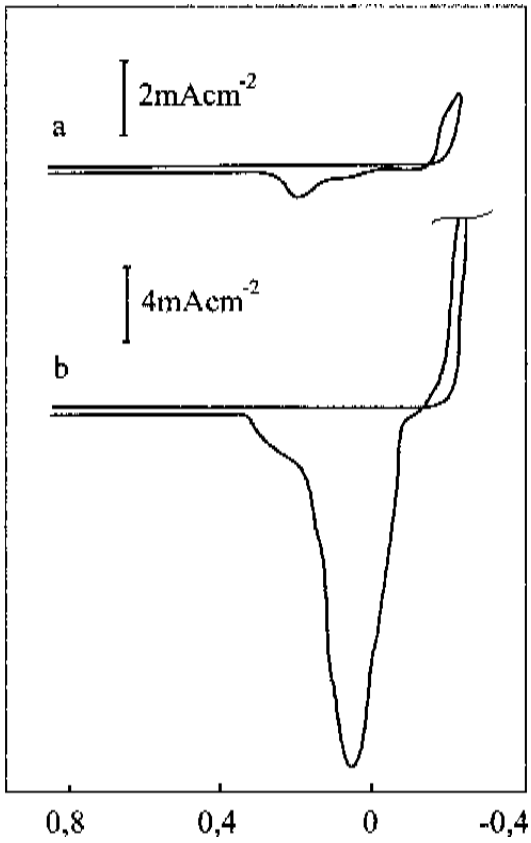

Fig. 1. Cyclic voltammograms in the aluminium electrolyte (0.935 M Al_2Br_6 ·DMEPAB solution in toluene) with 4.1 mM $Zr(Acac)_4$. Scan rate 20 mV s^{-1}; the potential scan to –200 (*a*) and –300 (*b*) mV

dox potential is considered to be more electropositive compared with that of aluminium calculated thermodynamically in aqueous solutions.

Which process, the electrodeposition of zirconium or that of aluminium, is the first cathodic process and which one is the second, may be elucidated with the aid of an analysis of the oxidation wave on a cyclic voltammogram.

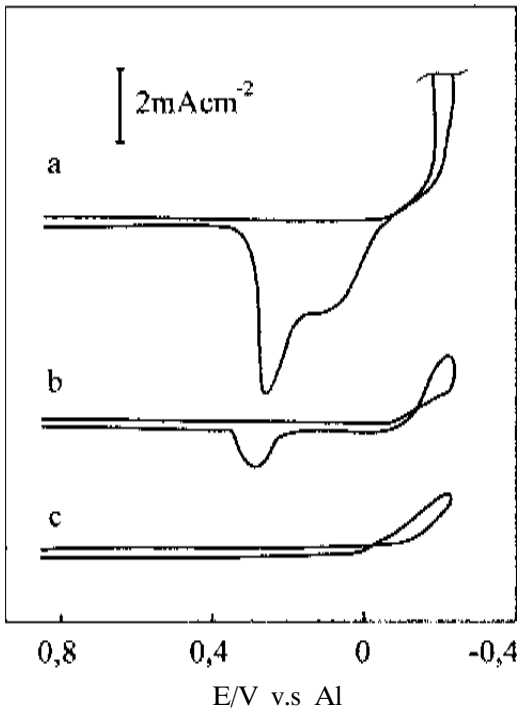

Fig. 2. Cyclic voltammograms in the aluminium electrolyte with 12.3 mM $Zr(Acac)_4$. The potential scan to –300 mV; scan rate: 20 (*a*), 50 (*b*) and 100 (*c*) mV s^{-1}

As is evident from Fig. 1, when the potential scanning is reversed at early stages of the deposition process, the anodic wave at 0.1–0.3 V is revealed. It is located in the region of more positive potentials in comparison to the oxidation potential of aluminium in $AlBr_3$-DMEPAB melts solutions in toluene. So, this anodic wave may be attributed to the reoxidation of zirconium, considering that the stripping electrodeposits consist only of aluminium and zirconium.

When the forward potential scanning is extended to more negative values, the height of this wave rises and at the same time the second anodic wave at 0–0.2 V appears, often merging with the first one. This second reoxidation wave corresponds to the oxidation potential of aluminium, defined repeatedly in aluminium electrolytes of various composition [15].

As may be inferred from a comparison of data in Fig. 1 with those in Fig. 2, the reoxidation maximum on the reverse potntial scan voltammogram in the region of 0.3 V increa-

Table. **Microanalysis data on electrodeposits obtained in $AlBr_3$-DMEPAB melt solutions in toluene with the addition of zirconium salts**

Zirconium salt	Concentration, mM	Current density, mA cm^{-2}	Deposition time, min	Deposit composition, wt. %	
				Zr	Al
$Zr(Acac)_4$	4.1	2.5	192	0.11	99.89
	4.1	5.0	96	0.02	99.98
	4.1	10.0	48	0.02	99.98
	8.2	2.5	192	6.11	93.89
	8.2	5.0	96	4.64	95.36
	8.2	10.0	48	4.58	95.42
ZrF_4	36	2.5	192	14.79	85.21
	36	5.0	96	11.30	88.70
	60	10.0	48	8.03	91.97
$ZrCl_4$	8.5	10.0	48	0.16	99.84

ses as the concentration of zirconium ions increases. This fact substantiates the above-mentioned supposition that this first anodic wave is attributed to the zirconium reoxidation.

It may be conceived alternatively that this anodic wave is due to the oxidation of acetylacetonate ions. However, this wave is absent, and solely the second one attributed to the aluminium reoxidation is found in the $AlBr_3$-DMEPAB melt solutions in toluene with the addition of acetylacetone up to 160 mM as well as with the addition of aluminium acetylacetonate up to 60 mM. This fact is an added reason for attributing the anodic wave in the region of 0.2–0.3 V to the reoxidation of zirconium.

A comparison of electric charges involved in the cathodic and anodic processes lends credence to the view that the anodic process results from the electrolytic reoxidation of electrodeposits and not from the oxidation of any component of the solution. When the concentration of $Zr(Acac)_4$ is less than 10 mM, the ratio of the anodic charge to the cathodic charge received by integrating the areas between the curves of the voltammogram and the ordinate is close to 1 (approximately 0.9–0.95). This ratio tends to diminish with the concentration of $Zr(Acac)_4$ in solution and becomes equal to about 0.7 when the zirconium concenration reaches 40 mM. It seems that the electrolytic dissolving of zirconium–aluminium electrodeposits during reverse (anodic) scan is accompanied by partially mechanical crumbling of metallic particles from the electrode.

Such a situation when the reoxidation of zirconium takes place at a more positive potential in comparison with that of aluminium suggests that zirconium deposits at a less negative potential than does aluminium. In other words, the electrodeposition of zirconium is the first cathodic process, whereas the electrodeposition of aluminium is the second one.

As is obvious from Fig. 3, when the potential sweep is extended sequentially to more negative values, the reoxidation wave of zirconium rises progressively and at the same time the reoxidation wave of aluminium appears (in the region of 0–0.2 V), increases and finally becomes predominant. A phenomenon of this kind is in excellent agreement with the mentioned proposition about the sequence of cathodic processes as well as with the data of Table about the composition of the electrodeposits.

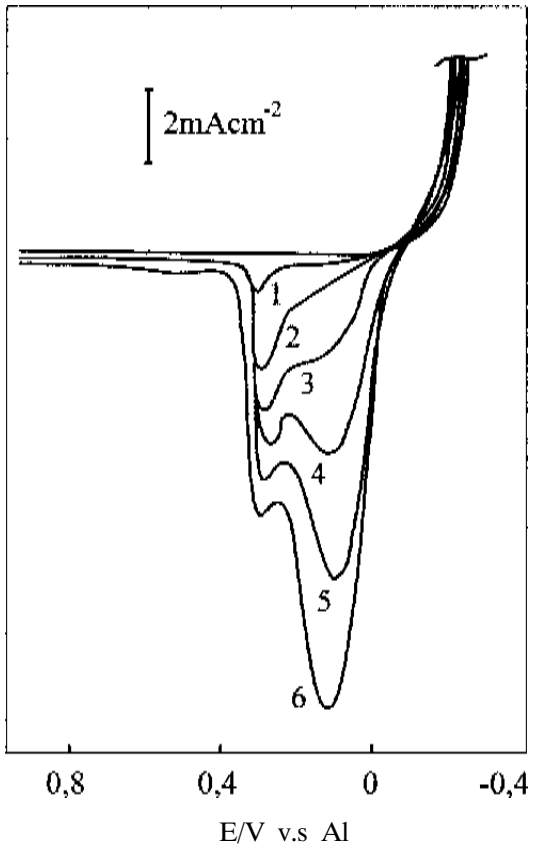

Fig. 3. Cyclic voltammograms in the aluminium electrolyte with 16.4 mM $Zr(Acac)_4$. Scan rate 20 mV s^{-1}; the potential scan to minus 200 (*1*), 300 (*2*), 320 (*3*), 340 (*4*), 360 (*5*) and 380 (*6*) mV

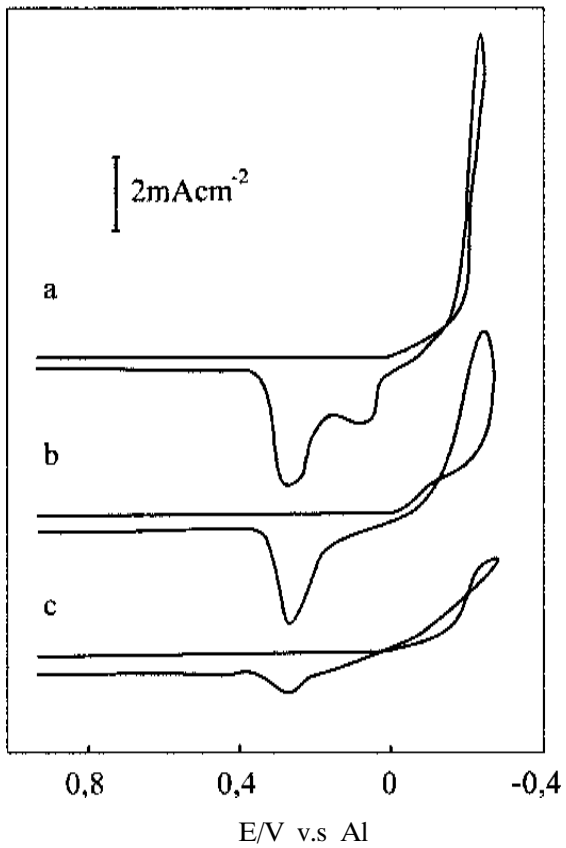

Fig. 4. Cyclic voltammograms in the aluminium electrolyte with 24 mM ZrF_4. The potential scan to –360 mV; scan rate: 20 (*a*), 50 (*b*) and 100 (*c*) mV s^{-1}

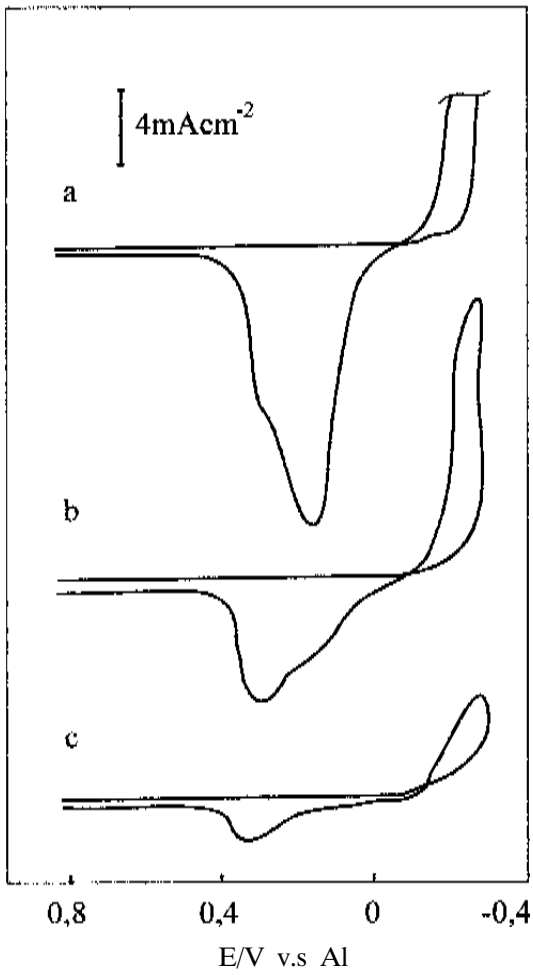

Fig. 5. Cyclic voltammograms in the aluminium electrolyte with 9.8 mM $ZrBr_4$. The potential scan to –350 mV; scan rate: 20 (*a*), 50 (*b*) and 100 (*c*) mV s^{-1}

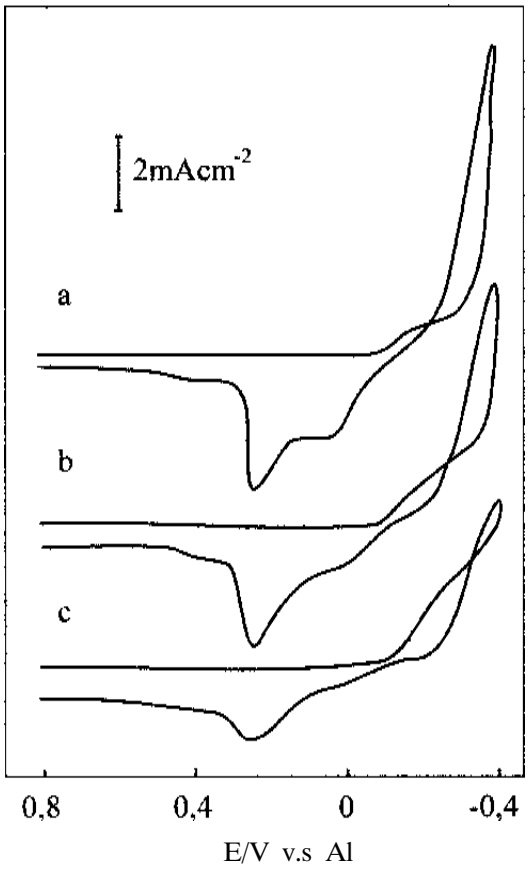

Fig. 6. Cyclic voltammograms in the aluminium electrolyte with 20 mM ZrJ_4. The potential scan to –400 mV; scan rate: 20 (*a*), 50 (*b*) and 100 (*c*) mV s^{-1}

When $Zr(Acac)_4$ in solution is replaced by zirconium halides, the cyclic voltammograms have in principle the same shape (Figs. 4–6), *i.e.*, when the potential sweep is extended sequentially to more negative values, it appears on the reverse scan at first as the reoxidation wave of zirconium in the region of 0.2–0.4 V, and only thereafter the reoxidation wave of aluminium appears in the region of 0–0.2 V. In the meantime, a sole reduction wave of both metals is observed on the cathodic part of the voltammogram.

Summarizing all the foregoing data, the following conclusions can be done with a fair degree of assurance. Although no distinct reduction waves are observed for the electrodeposition processes of zirconium and aluminium, and thus both these metals deposit in the same very close potential range, an analysis of changes in the deposits composition and features of sequence of anodic processes suggests that zirconium deposition is the first cathodic process starting at a less negative, even if extremely insignificantly, potential in comparison to aluminium whose deposition is the second cathodic process starting at a more negative potential. Contrastingly, zirconium and aluminium electrochemical oxidation takes place at rather different potentials, and distinct oxidation waves can be observed for each metal.

As is seen in all the foregoing figures, the cyclic voltammograms display a "nucleation loop" after a scan reserval in the cathodic region. It is common knowledge that this indicates that the metal deposition requires an overpotential in order to initiate the nucleation and growth of deposit. This assumption is supported by a typical shape of current–time transients in the potential region of zirconium codeposition with aluminium: a current spike and subsequent broad current maximum (Fig. 7).

As may be inferred from measurements at less negative potentials where most likely zirconium solely reduces on the cathode, the current–time transients have a shape characteristic of diffusion-controlled processes. The diffusion coefficient of zirconium ions calculated using Cottrell plots of i *vs* $t^{-1/2}$ was found to be $D = 1.5 \times 10^{-7}$ cm^2 s^{-1} in 16.4 mM $Zr(Acac)_4$ solutions and $D = 1.75 \times 10^{-7}$ cm^2 s^{-1} in 20 mM ZrJ_4 solutions, whereas the diffusion coefficient for alumi-

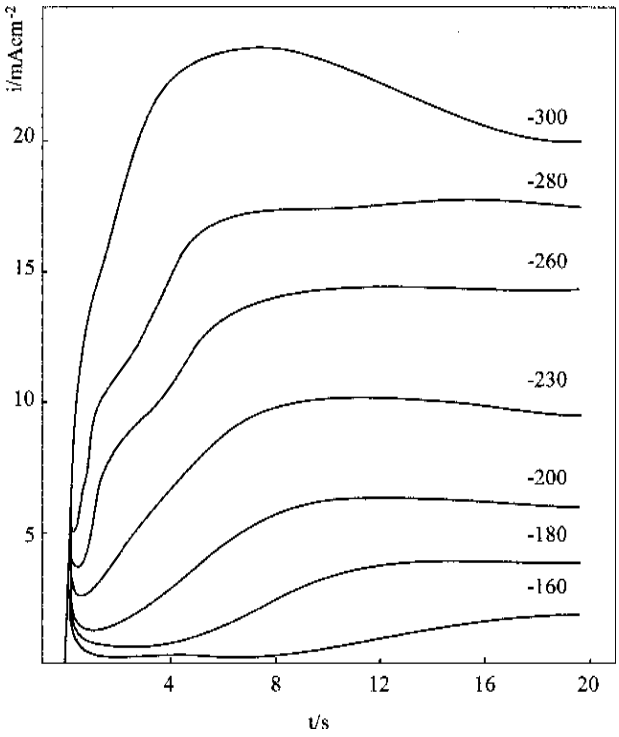

Fig. 7. Potentiostatic current-time transients for the codeposition of Zr with Al from aluminium electrolyte with 8.2 mM $Zr(Acac)_4$ at potentials indicated (in mV)

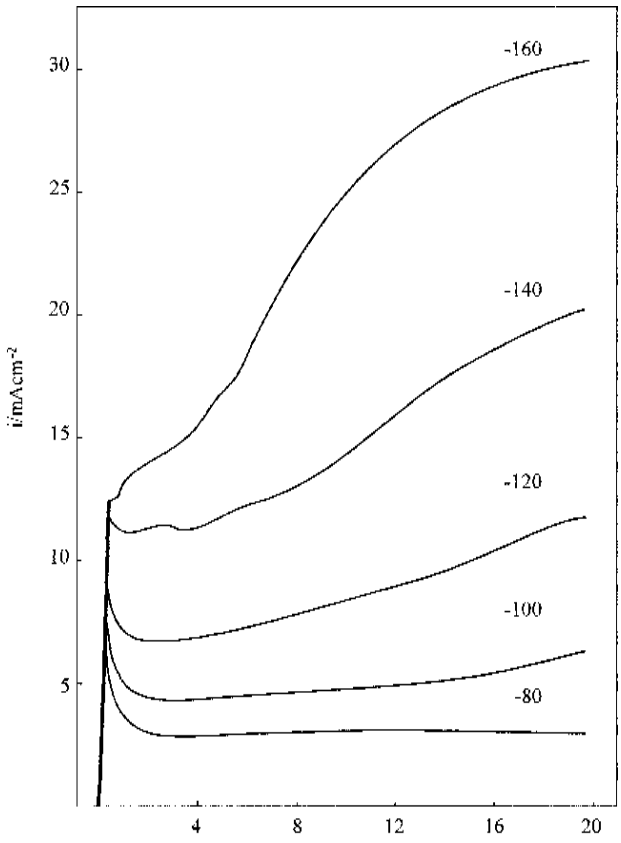

Fig. 9. Potentiostatic current-time transients for the codeposition of Zr with Al from aluminium electrolyte with 8.6 mM $ZrCl_4$ at potentials indicated (in mV)

nium ions was obtained earlier [16] as $D = (1.1 \pm \pm 0.4)$ x 10^{-6} cm^2 s^{-1}.

Previously [16] we have demonstrated that the electrodeposition process of pure aluminium from $AlBr_3$ -DMEPAB solutions in toluene without any addition ions involves progressive nucleation with a diffusion-controlled growth of three-dimensional nuclei. As will be apparent from Fig. 8, the results of voltammetric measurements in the aluminium electrolyte with the addition of zirconium ions more adequately depict the instantaneous nucleation or at least suggest an intermediate model between instantaneous and progressive nucleation, as they are defined theoretically in [17].

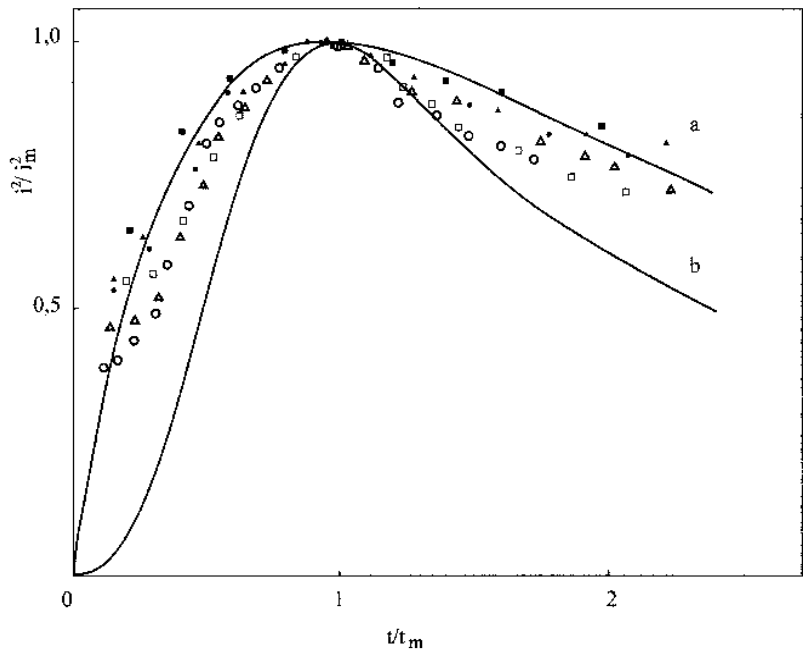

Fig. 8. Comparison of the dimentionless experimental data for the codeposition of Zr with Al from aluminium electrolyte with 8.2 mM $Zr(Acac)_4$ derived from current-time transients at –260 (○), –280 (Δ) and –300 (□) mV and with 24 mM ZrF_4 at –320 (•), -330 (▲) and –350 (■)mV

As is seen in Fig. 7, the current–time transients received at more negative potentials disclose as though a double current maximum. This phenomenon is more obvious in $ZrCl_4$ solutions (Fig. 9). Similar current-time transients were considered also in the case of codeposition of aluminium with zinc [16]. One may suggest that the first vague maximum is due to zirconium nucleation and

the second one to aluminium nucleation and growth. However, the regularities of the concurrent deposition process of two metals remain to be studied.

CONCLUSIONS

1. A decrease of the zirconium amount with decreasing the zirconium concentration and increasing the current density was determined in electrodeposits obtained from $AlBr_3$-dimethylethylphenylammonium bromide melt solutions in toluene with the addition of zirconium salts.

2. The deposition processes of zirconium and aluminium proceeded at extremely close potentials, the deposition of zirconium being the first electrode process and that of aluminium the second one.

3. Although no distinct reduction waves for zirconium and aluminium became apparent on cyclic volmammograms, there are well-defined separated oxidation waves on a reverse scan of the potential.

4. Examination of the initial stages of the deposition process suggests most likely an intermediate model between instantaneous and progressive nucleation.

Received 28 December 2000
Accepted 1 February 2001

References

1. N. Holstein, K. Jüttner, M. Kupper and H. Lowe, *Galvanotechnik*, **90**, 480 (1999).
2. R. T. Carlin, P. C. Trulove and H. C. De Long, *J. Electrochem. Soc*., **143** (9), 2747 (1996).
3. J. A. Mitchell, W. R. Pitner, C. L. Hussey and G. R. Stafford, *J. Electrochem. Soc*., **143**(11), 3448 (1996).
4. R. T. Carlin, H. C. De Long, J. Fuller and P. C. Trulove, *J. Electrochem. Soc*., **145**(5), 1598 (1998).
5. L. Simanavičius, A. Stakėnas and A. Šarkis, *Chemija* (Vilnius), N 3, 60 (1997).
6. M. R. Ali, A. Nishikata and T. Tsuru, *Electrochim. Acta*, **42**(12), 1819 (1997).
7. J. S.-Y. Liu, P. Y. Chen, J.-W. Sun and C. L. Hussey, *J. Electrochem. Soc*., **144**(7), 2288 (1997).
8. T. P. Moffat, *J. Electrochem. Soc*. **141**(9), L115 (1994).
9. 5. L. Simanavičius, A. Stakėnas, A. Šarkis and E. Matulionis, *Chemija* (Vilnius), **10** (3), 209 (1999).
10. A. Šarkis, A. Stakėnas and E. Matulionis, *Chemija* (Vilnius), N 4, 43 (1996).
11. W. R. Pitner, C. H. Hussey and G. R. Stafford, *J. Electrochem. Soc*., **143**(1), 130 (1996).
12. G. R. Stafford, *J. Electrochem. Soc*., **141**(4), 945 (1994).
13. A. J. Bard, R. Parsons and J. Jordan, *Standard Potentials in Aqueous Solutions*, Dekker Inc., N. Y.-Basel (1985).
14. *Handbook of Inorganic Preparative Chemistry* (in Russian) (Ed. by G. Brauer), p. 634, IL, Moscow (1956).
15. L. Simanavičius, A. Stakėnas and A. Šarkis, *Electrochim. Acta*, **46**, 499 (2000).
16. L. Simanavičius, A. Stakėnas and A. Šarkis, *Electrochim. Acta*, **42**, 1581 (1997).
17. B. Scharifker and G. Hills, *Electrochim. Acta*, **28**(7), 879 (1983).

A. Stakėnas, L. Simanavičius, A. Šarkis, E. Matulionis

CIRKONIO SĄSĖDIS SU ALIUMINIU IŠ $AlBr_3$-DIMETILETILFENILAMONIO BROMIDO TIRPALŲ TOLUENE

S a n t r a u k a

Nustatyta, kad dangose, gautose iš $AlBr_3$-dimetiletilfenilamonio bromido lydalo tirpalų toluene su cirkonio druskų priedais, cirkonio kiekis mažėja mažėjant cirkonio koncentracijai tirpale ir didėjant srovės tankiui. Cirkonio ir aliuminio skyrimosi potencialai yra be galo artimi, bet galima padaryti išvadą, kad cirkonis pradeda skirtis teigiamesnių potencialų srityje negu aliuminis. Ciklinėse voltamperinėse kreivėse nematyti atskirų cirkonio ir aliuminio redukcijos bangų, tačiau skleidžiant potencialą atgaline kryptimi registruojamos aiškios atskiros šių metalų oksidacijos bangos. Pradinių elektrolitinio nusodinimo stadijų ant inertinio platinos katodo tyrimai rodo, kad geriausiai kristalizacijos procesą atspindi tarpinis modelis tarp akimirksninės ir progresuojančios nukleacijos.

А. Стакенас, Л. Симанавичюс, А. Шаркис, Э. Матулёнис

СООСАЖДЕНИЕ ЦИРКОНИЯ С АЛЮМИНИЕМ ИЗ РАСТВОРОВ $AlBr_3$-БРОМИДА ДИМЕТИЛЭТИЛФЕНИЛАММОНИЯ В ТОЛУОЛЕ

Р е з ю м е

Определено, что количество циркония в электролитических покрытиях, осажденных из толуольных растворов расплава $AlBr_3$-бромид диметилэтилфениламмония с добавками солей циркония, уменьшается со снижением концентрации циркония в растворе и увеличением плотности тока. Потенциалы выделения циркония и алюминия крайне близки, однако можно сделать вывод, что цирконий выделяется при более положительных потенциалах, чем алюминий. На циклических вольтамперных кривых отсутствуют отдельные волны восстановления циркония и алюминия, тем временем при обратной развертке потенциала обнаруживаются ясные отдельные волны окисления этих металлов. Изучение начальных стадий электроосаждения на инертном платиновом катоде показывает, что процесс кристаллизации, вероятнее всего, соответствует промежуточной модели нуклеации между моментной и прогрессирующей.